Spring 2012

A Synthetic Study and Preliminary Evaluation of a Protease-Activated Doxazolidine Prodrug

Sean Colvin
University of Colorado Boulder

Chemistry and Biochemistry Honors Thesis

Spring 2012

A Synthetic Study and Preliminary Evaluation of a Protease-Activated Doxazolidine Prodrug

by

Sean M. Colvin

Thesis Advisor:

Dr. Tad H. Koch

(Department of Chemistry and Biochemistry)

Committee Members:

Dr. Hubert Yin

(Department of Chemistry and Biochemistry)

Charles Doersch

(Program for Writing and Rhetoric)

Contents

Acknowledgements

First, I would like to express my utmost appreciation to Dr. Tad H. Koch for providing me with both the opportunity to take on this project and his unreserved guidance. I am forever a more enriched scientist and person because of it.

I also would like to acknowledge Dr. Ben Barthel and Price Kirby for their daily mentoring, support, and patience in my development as a scientist, through both my success and repeated failures.

Additionally, I want to thank Vivek Chadayammuri, Alexander Rowan, and Daniel Rudnicki for making my time in the Koch lab both enjoyable and intellectually stimulating.

Finally, I am wholeheartedly grateful for the support of my mother, father, and sister, who have been unconditional sources of encouragement throughout my life.

Abstract

Described are studies focused on prodrug delivery of a doxorubicin-formaldehyde conjugate, doxazolidine (Doxaz). Designed for targeted activation by the serine protease plasmin, Protease-Activated Doxazolidine (PAD) embodies a new approach to selective cancer treatment. Following a model developed by the Koch laboratory, the PAD prodrug consists of a peptide tag attached to Doxaz via a self-eliminating spacer. Enzymatic cleavage of the peptide and subsequent spacer elimination results in release of active Doxaz into the tumor environment from the otherwise inactive prodrug. Problems in the current synthesis of PAD are addressed in steps taken towards a new synthetic pathway. Additionally, this study addresses preliminary biological evaluation of PAD activation and treatment feasibility through multiple enzyme and cancer cell assays. Finally, this work addresses the specific role of the plasmin system in PAD activation through RNA interference. Using short hairpin RNA to knockdown key components of the plasmin activation pathway, a more accurate portrayal of the plasmin system's role in PAD activation can be attained. Results suggest PAD is a feasible drug candidate and offer encouragement for advanced evaluation as a novel therapeutic.

Introduction

Since the 1970s, the anthracycline doxorubicin (Dox, Adriamycin; Figure 1) has been a mainstay in cancer treatment. First isolated from the soil microbe *Streptomyces peucetius*, Dox exhibits significant antitumor activity against a variety of cancer types.[1-3] As with many cancer therapeutics, Dox treatment is hampered by adverse side effects, the most notable of which is irreversible cardiotoxicity.[4] In addition, acquired tumor resistance further limits clinical success.[4] Because of these problems, much research has been conducted to elucidate the cytotoxic mechanisms of Dox-caused death to cancer cells and healthy heart cells. The exact mechanisms still remain unclear; however, the anticancer mechanism of Dox is known to be topoisomerase II (TOP2) dependent, whereas Dox cardiotoxicity is thought to stem from induction of reactive oxygen species.[5]

Discovered by the Koch laboratory, doxazolidine (Doxaz), is a formaldehyde conjugate of Dox, in which a methylene group bridges the oxygen and nitrogen of the daunosamine, forming an oxazolidine (Figure 1, methylene highlighted in red).[6] The addition of another equivalent of formaldehyde leads to formation of a Doxaz dimer, doxoform (DoxF), which has been shown to act as Doxaz prodrug.[6] Despite differing from Dox by just a single atom, Doxaz

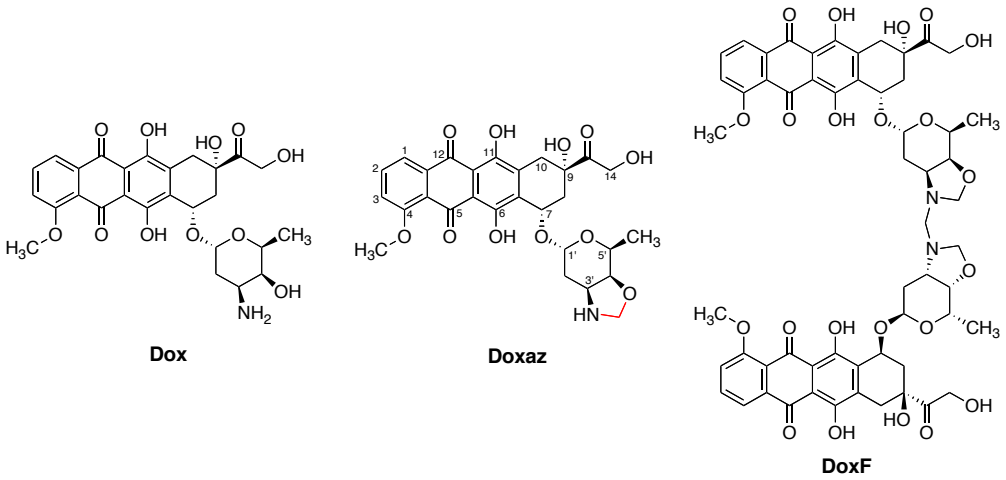

Figure 1. Structures of doxorubicin (Dox), doxazolidine (Doxaz), and doxoform (DoxF). Highlighted in red on Doxaz is the single methylene difference.

exhibits a superior therapeutic profile than that of Dox. Doxaz inhibits cancer cell growth with 100-10,000 times the efficacy of Dox, including notable activity against Dox resistant cell lines.[6] While Doxaz displays this greater antitumor potency, treatment of rat cardiomyocytes does not result in increased toxicity relative to Dox.[6]

There is a fundamental explanation of the differences between Doxaz and Dox. The mechanism by which Doxaz triggers cell death is inherently different than that of Dox. Doxaz is topoisomerase II independent; instead, it forms a virtual cross-link across 5'-GC-3' DNA base pairs (Figure 2).[6-7] Because of this, Doxaz is better considered as a new therapeutic rather than an improved Dox.

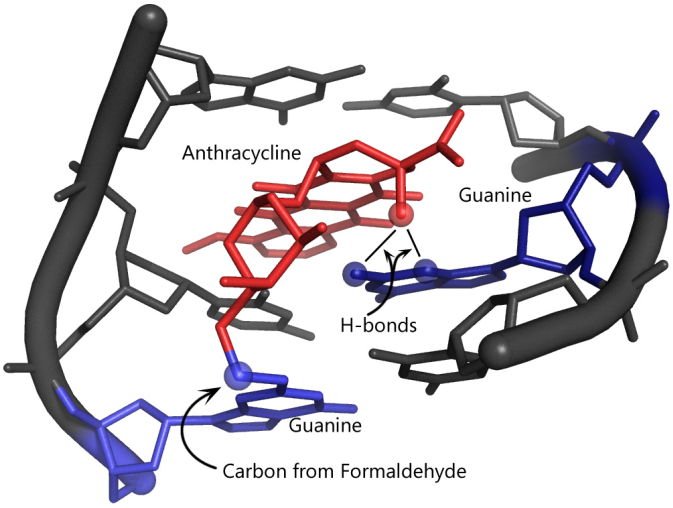

Figure 2. Virtual cross-link of DNA by Doxaz. Figure courtesy of Dr. Ben Barthel.

With a distinct mechanism and favorable therapeutic profile, Doxaz is an attractive new drug; however, a conventional approach to Doxaz treatment is not feasible. In aqueous solution, Doxaz is rapidly hydrolyzed to Dox with a half-life of three minutes.[6] This problem is alleviated using a prodrug strategy, in which an inactive form of a therapeutic is activated *in vivo* to release the active form at a specific location. High potency and a short half-life make Doxaz an ideal candidate for prodrug delivery. This approach also allows for greater tumor specificity with proper prodrug design.

Employing the prodrug strategy, the Koch group recently described a pentyl carbamate prodrug of Doxaz, pentyl-PABC-Doxaz (PPD, Figure 3), designed for enzymatic activation by carboxylesterase 2 (CES2).[8] The drug produced favorable results in animal trials, exhibiting

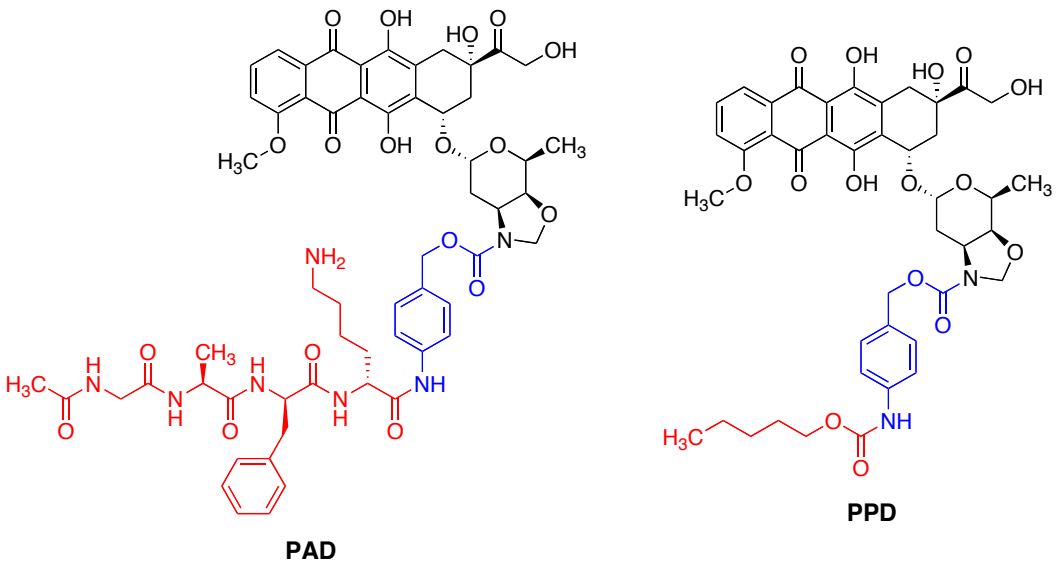

Figure 3. Structures of Doxaz prodrugs Ac-GaFK-PABC-Doxaz (PAD, left), pentyl-PABC-Doxaz (PPD, right). Highlighted in red are the enzymatic specific tags, and in blue are the self-eliminating spacers.

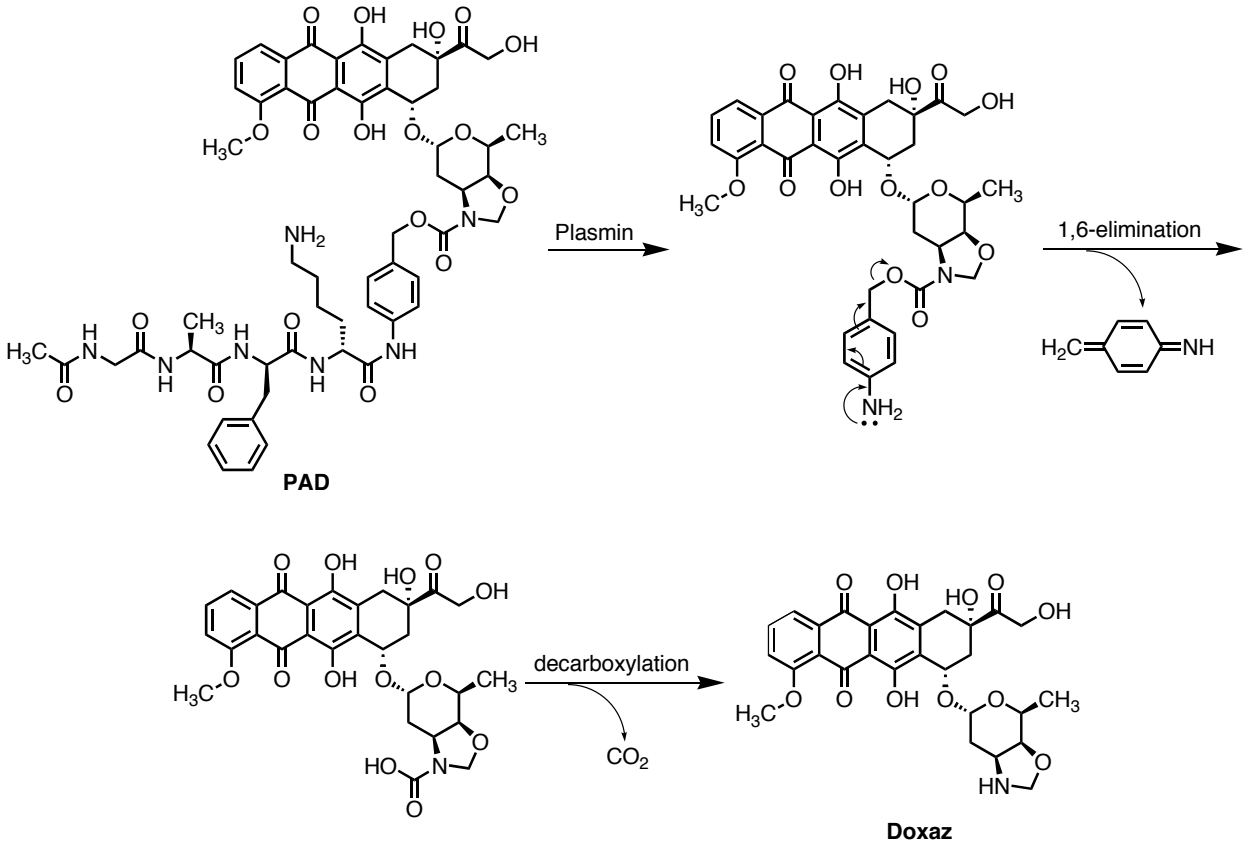

Scheme 1. Proposed PAD activation pathway via the protease plasmin.

substantial tumor growth inhibition in mice; furthermore, prodrug treatment displayed significantly lower signs of cardiotoxicity in the test mice at higher doses relative to Dox.[9]

These positive results buoy a generic model for Doxaz prodrugs, in which a tag for targeted activation is attached to Doxaz using a self-eliminating spacer. This provides versatility in treating different tumor types. Following this model, another enzyme-activated prodrug has been developed for targeted activation by the protease plasmin. Originally modeled after aFK-Dox designed by de Groot et al.,[10] Ac-GaFK-PABC-Doxaz, or Protease-Activated Doxazolidine (PAD), consists of an N-acetyl glycine-D-alanine-L-phenylalanine-L-lysine (Ac-GaFK) tetrapeptide tag to a *p*-aminobenzyloxycarbonyl (PABC) spacer coupled to Doxaz (Figure 3). The protease plasmin is proposed to hydrolyze the bond between the peptide and spacer in the first step of activation (Scheme 1). Following a spontaneous 1,6 elimination of the spacer to release the iminoquinone methide and a subsequent spontaneous decarboxylation, Doxaz is liberated at the tumor site.

Plasmin is an ideal target enzyme for site-specific prodrug activation, as it is a hallmark of invasive cancers.[11] Involved in the breakdown of extracellular matrix proteins, plasmin is a crucial component of tumor proliferation and metastasis.[11] First secreted as the zymogen plasminogen, plasmin activation occurs at the cell surface via serine protease urokinase-type plasminogen activator (uPA).[11] The membrane tethered uPA receptor (uPAR) binds uPA to form an active complex which cleaves plasminogen to produce active plasmin (Figure 4).[11] The presence of inhibitors in the bloodstream limit plasmin proteolytic activity to tumor sites;[11] thus, unwanted prodrug activation in circulation is unlikely.

With plasmin established as a therapeutic target, PAD research in the Koch laboratory has been focused on multiple facets of drug development, the first of which being a scalable

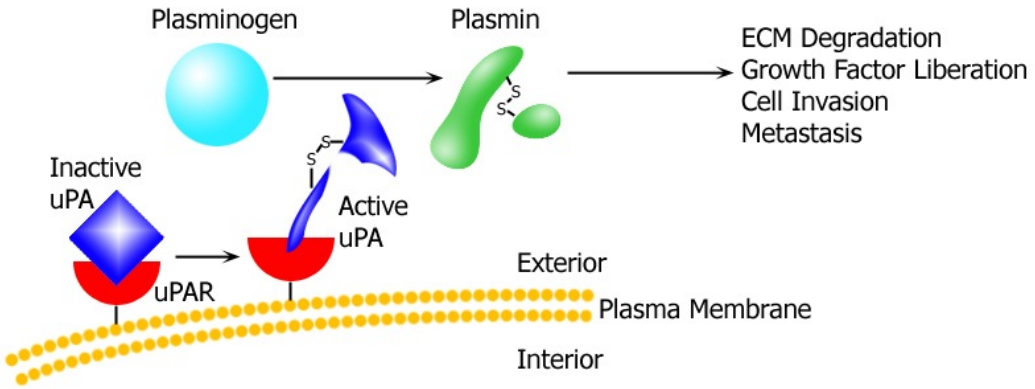

Figure 4. Urokinase-type plasminogen activator system. Figure courtesy of Dr. Ben Barthel.

synthesis. The current synthesis of PAD is hampered by a problematic deprotection of the final product, resulting in variable quality and loss of material. A new pathway is necessary for production of enough material for future animal studies. The first section of this thesis describes steps toward a key intermediate in a new PAD synthetic pathway.

The second prominent area of PAD research is one of preliminary evaluation. Enzyme kinetics and cell growth inhibition experiments provide proof of concept and a forecast of potential therapeutic success. The plasmin-PAD enzyme-substrate relationship was examined through timecourse and Michaelis-Menten kinetics. Drug activation and efficacy was further evaluated against multiple cell lines through various half maximal inhibitory concentration (IC_{50}) assays, employing exogenous plasmin and a panel of protease inhibitors.

The final aspect of PAD research presented here is an investigation of the role of endogenous plasmin activation in cells. Using short hairpin RNA (shRNA) mediated RNA interference (RNAi), both uPA and uPAR were targeted for knockdown in the cancer cell lines N-HepG2 (liver), which has shown 5-fold reduction of PAD response in the presence of aprotinin (Koch lab unpublished data), and DU-145 (prostate), which express moderate to high levels of both uPA and uPAR mRNA.[12-13] Knockdown cell lines were then to be assayed for PAD activation and efficacy through IC_{50} experiments.

These three elements of PAD research contribute to the overarching objective in doxazolidine research. Successful implementation of the prodrug strategy may lead to a new clinical therapeutic for a variety of invasive cancers.

References

1. Di Marco, A.; Gaetini, M.; Scarpinato, B. Adriamycin (NSC-123, 127): a new antibiotic with antitumor activity. *Cancer Chemother. Rep.* **1969**, *53*, 33-37.
2. Arcamone, F.; Cassinelli, G.; Fantini, G.; Grein, A.; Orezzi, P.; Pol, C.; Spalla, C. Adriamycin, 14-hydroxydaunomycin, a new antitumor antibiotic from *S. peucetius* var. *caesius*. *Biotechnol. Bioeng.* **1969**, *11*, 1101-1110.
3. Young, R. C.; Ozols, R. F.; Myers, C. E. Medical progress: the anthracycline antineoplastic drugs. *New Engl. J. Med.* **1981**, *305*, 139-153.
4. Menna, P.; Salvatorelli, E.; Gianni, L.; Minotti, G. Anthracycline cardiotoxicity. *Top Curr Chem*. **2008**, *283*, 21-44.
5. Pommier, Y. DNA Topoisomerases and Their Inhibition by Anthracyclines. *Anthracycline Antibiotics: New Analogues, Methods of Delivery, and Methods of Action*; American Chemical Society: Washington, DC, 1995, pp 183-203.
6. Post, G. C.; Barthel, B. L.; Burkhart, D. J.; Hagadorn, J. R.; Koch, T. H. Doxazolidine, a proposed active metabolite of doxorubicin that cross-links DNA. *J. Med. Chem.* **2005**, *48*, 7648-7657.
7. Kalet, B. T.; McBryde, M. B.; Espinosa, J. M.; Koch, T. H. Doxazolidine induction of apoptosis by a topoisomerase II independent mechanism. *J. Med. Chem.* **2007**, *50*, 4493-4500.
8. Burkhart, D. J.; Barthel, B. L.; Post, G. C.; Kalet, B. T.; Nafie, J. W.; Shoemaker, R. K.; Koch, T. H. Design, synthesis, and preliminary evaluation of doxazolidine carbamates as prodrugs activated by carboxylesterases. *J. Med. Chem.* **2006**, *49*, 7002-7012.

9. Barthel, B. L.; Zhang, Z.; Rudnicki, D. L.; Coldren, C. D.; Polinkovsky, M.; Sun, H.; Koch, G. G.; Chan, D. C. F.; Koch, T. H. Preclinical efficacy of a carboxylesterase 2-activated prodrug of doxazolidine. *J. Med. Chem.* **2009**, *52*, 7678-7688.
10. de Groot, F. M. H.; de Bart, A. C. W.; Verheijen, J. H.; Scheeren, H. W. Synthesis and biological evaluation of novel prodrugs of anthracyclines for selective activation by the tumor-associated protease plasmin. *J. Med. Chem.* **1999**, *42*, 5277-5283.
11. Andreasen, P. A.; Kjøller, L.; Christensen, L; Duffy, M. J. The urokinase-type plasminogen activator system in cancer metastasis: a review. *Int. J. Cancer* **1997**, *72*, 1-22.
12. Plasminogen activator, urokinase mRNA. National Cancer Institute – Developmental Therapeutics Program. http://dtp.nci.nih.gov/mtweb/targetinfo?moltid=GC31606&moltnbr=31605
13. Plasminogen activator, urokinase receptor mRNA. National Cancer Institute Developmental Therapeutics Program. http://dtp.nci.nih.gov/mtweb/targetinfo?moltid=GC19033&moltnbr=9631

Results and Discussion

1. Steps Towards the Synthesis of PAD

In the current synthesis of PAD, a late-stage deprotection of the lysine residue in the peptide results in complicated purification and poor yield. The anthracycline moiety is prone to side reactions under many deprotection conditions, resulting in a convoluted mixture of products. An ideal PAD synthesis would allow for deprotection of the peptide prior to coupling with Doxaz. Described here are steps towards such a synthesis.

From Scheme 2, diazotization followed by displacement with azide converted commercially available *p*-aminobenzyl alcohol, **1**, to azide **2** in 83% yield. Carbonate **3** was isolated in 66% yield upon reaction of **2** with 4-nitrophenyl chloroformate. Degradation of **3** on silica was observed, likely resulting in the majority of observed product loss.

Conversion of Dox•HCl to Doxaz via reaction of the free base with formaldehyde was almost quantitative (98%). ^{1}H NMR analysis suggested that upon concentration of the reaction mixture, excess formaldehyde present caused the formation of DoxF resulting in a 2:1 mixture of Doxaz/DoxF. Reaction of the mixture with carbonate **3** produced the desired azide **5** in 38% yield isolated by flash chromatography. The presence of both Doxaz and DoxF did not seem to hinder the reaction. We proposed that trace water in the reaction solvent preferentially hydrolyzed the DoxF dimer to 2 equiv. of Doxaz without significantly hydrolyzing Doxaz. Reaction progress determined by reverse-phase HPLC suggested near complete consumption of starting material to produce a single major product. In light of this evidence, low isolation yield is most likely attributed to anthracycline degradation on silica during flash chromatography. Strong streaking was observed, leaving the silica with a pink appearance regardless of solvent system polarity. Isolation by HPLC may prove a better alternative.

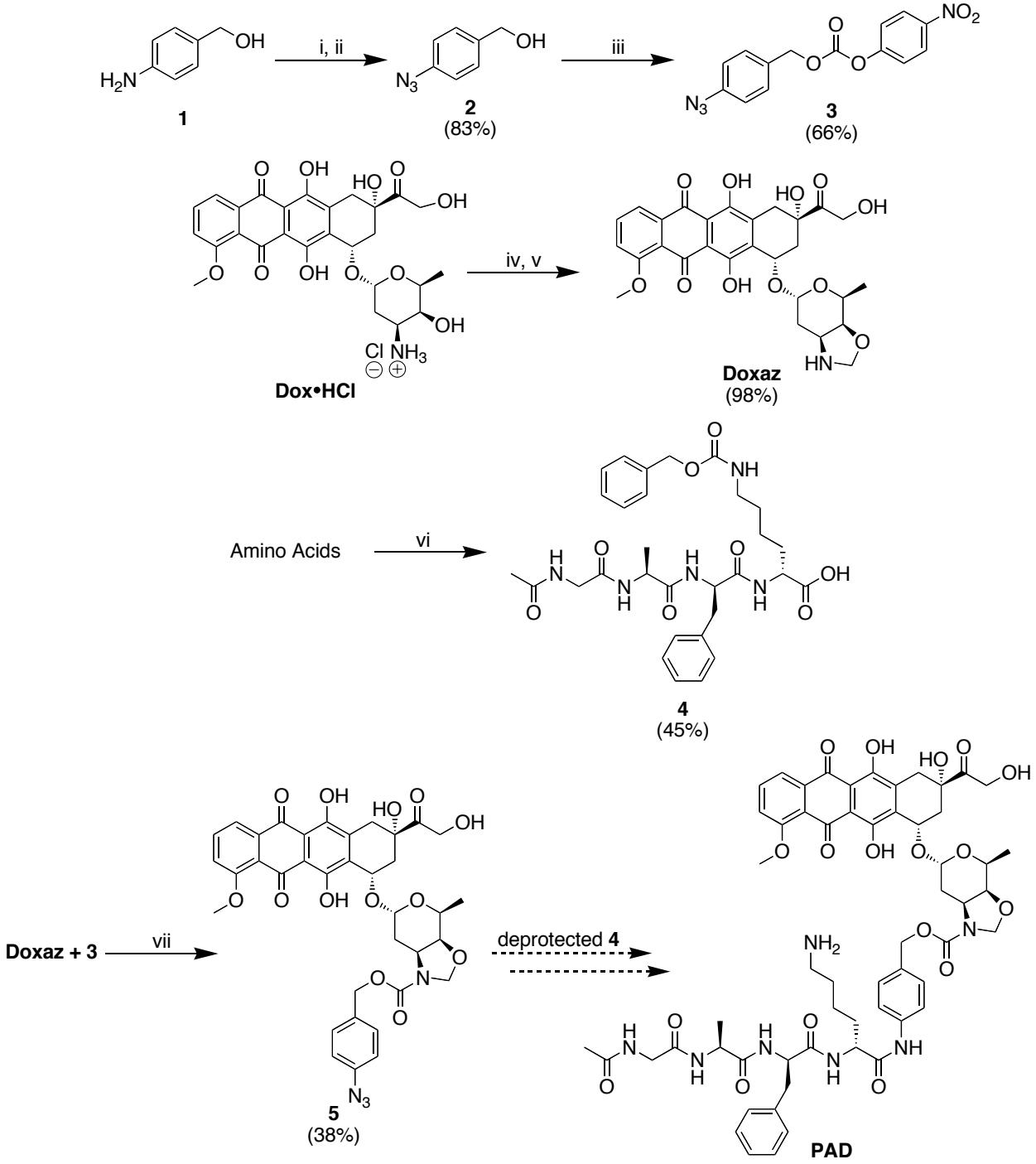

Scheme 2. PAD synthesis pathway. (i) $NaNO_2$, HCl, 0 °C; (ii) NaN_3, 0 °C; (iii) 4-nitrophenyl-chloroformate, pyridine, rt; iv) $NaHCO_3$ 4 °C; (v) paraformaldehyde, rt; (vi) SPPS; (vii) 40 °C.

Peptide **4** was synthesized using solid phase peptide synthesis from Fmoc-Lys(Z)-OH – where Z corresponds to a benzyloxycarbonyl side-chain protecting group – loaded on a 2-chlorotrityl resin. The tetrapeptide was recovered in 45% yield following cleavage from resin and isolation. Poor peptide solubility in organic solvents contributed to low yield.

With key intermediate **5** produced in a 20% overall yield across six steps in a straightforward, scalable manner, complete synthesis of PAD via this pathway is a foreseeable goal. Amidative coupling of azide **5** to the C-terminus of deprotected **4** should afford PAD. The early deprotection of **4**, in addition to optimization of preceding steps to boost the overall yield of intermediate **5**, should provide a pathway capable of producing ample material for biological studies.

2. Enzymatic and Cellular Studies with PAD

2.1 Enzyme Kinetics

Turning to preliminary evaluation of PAD, timecourse and Michaelis-Menten kinetics experiments show that Plasmin and PAD exhibit standard enzyme-substrate behavior (Figure 5).

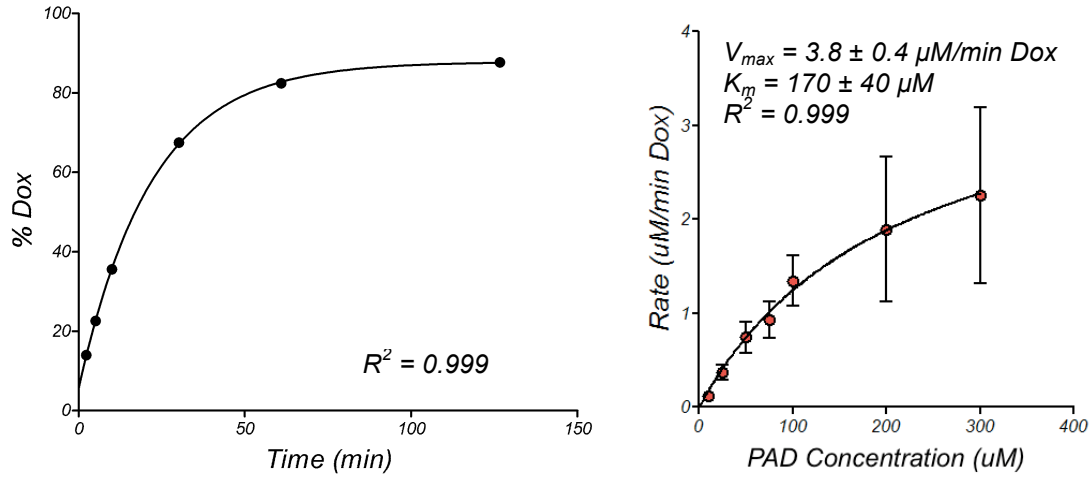

Figure 5. Plasmin-catalyzed PAD activation kinetics at 37 ºC. Timecourse kinetics (left) Michaelis-Menten kinetics (right).

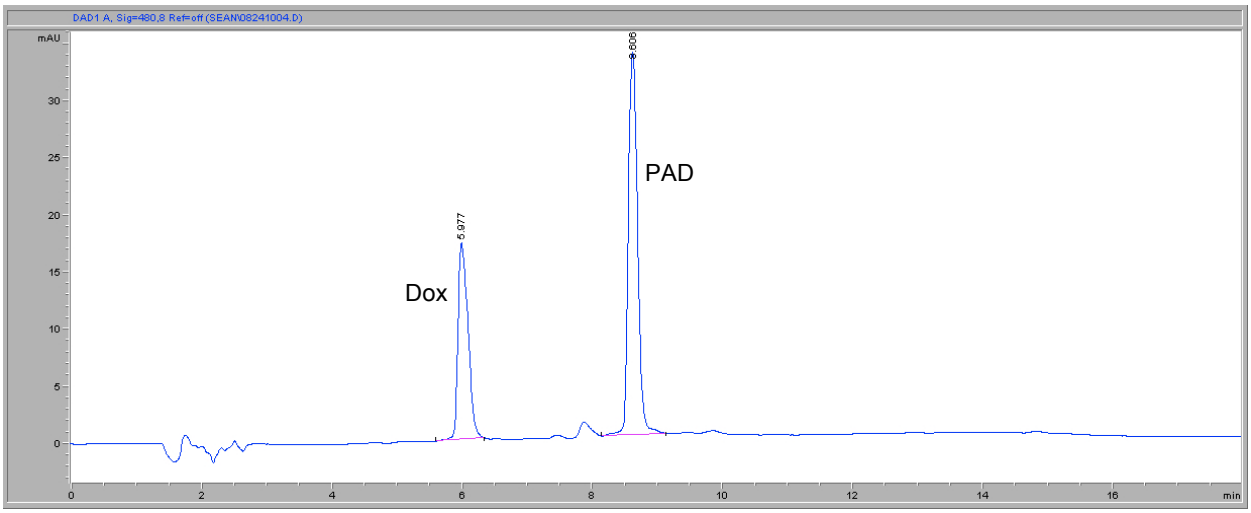

Figure 6. Representative HPLC chromatogram of enzymatic activation of PAD, with peaks corresponding to Dox and PAD labeled accordingly. Monitored at 480 nm.

The timecourse was evaluated as the production of Dox over time; because of the rapid hydrolysis of Doxaz to Dox, a direct measurement of Doxaz is difficult by HPLC. In the absence of plasmin, PAD is stable and no Doxaz is released; therefore, any Dox observed must be a result of enzymatic cleavage of the prodrug.

The presence of only two peaks in the 480 nm HPLC chromatogram (Figure 6) allows for simple determination of percent conversion. The percentage of the Dox peak (~6 min) relative to the prodrug peak (~9 min) is directly indicative of percent conversion, since all unstable intermediates, including those formed between enzyme hydrolysis and release of Doxaz, are too short-lived to see by HPLC. In this experiment, plasmin catalyzed conversion of PAD to Doxaz – and subsequent hydrolysis to Dox – is shown to approach completion (88%) within 2.5 h, representing fast and efficient enzymatic turnover.

Using the same analysis, plasmin PAD activation is shown to fit the standard Michaelis-Menten model with observed V_{max} and K_m values of 3.8 ± 0.4 μM Dox min^{-1} and 170 ± 40 μM PAD, respectively; however, such behavior was not initially apparent. Previous Michaelis-Menten kinetics experiments employing high concentrations of acidic buffer in the drug

formulation resulted in an observed inhibitory effect at high concentrations. Relative plasmin activity notably decreased at PAD concentrations above 100 μM, rather than the leveling off expected when approaching V_{max}. Experiments employing formulated PAD containing saline and 10% PEG-400 did not reproduce the observed inhibition, and instead displayed the Michaelis-Menten described above. Because formulated drug will be used in more advanced studies, such as animal experiments, the obtained kinetics are most relevant to current research.

2.2 Cancer Cell Growth Inhibition Studies

With this evidence for enzyme-catalyzed activation, PAD-induced cancer cell growth inhibition can be explored. PAD alone was shown to be quite effective in inhibiting growth in BxPC3 (pancreatic), MiaPaCa2 (pancreatic), and SHP77 (small-cell lung) cancer cell lines, with IC_{50} values in the micromolar and nanomolar levels (Table 1). PAD efficacy increased by more than an order of magnitude in the presence of exogenous plasmin, confirming the release of a more potent cytotoxic agent, Doxaz. This result serves as precedent for PAD activation to Doxaz by plasmin in complex systems.

A more puzzling discovery made by Dr. Barthel of the Koch lab, is PAD efficacy appears to be unaffected by the presence of a known plasmin inhibitor aprotinin. This result suggests PAD activation may occur by alternative avenues, prompting a closer examination of PAD activation in cell culture.

Treatment	$\log IC_{50}$		
	BxPC3	MiaPaCa2	SHP77
PAD	-6.39 ± 0.04	-6.62 ± 0.03	-5.80 ± 0.03
PAD + Plasmin	-7.8 ± 0.3	-7.96 ± 0.07	-7.53 ± 0.05
PAD + Aprotinin[a]	-6.3 ± 0.1	-6.56 ± 0.03	—

Table 1. IC_{50} values expressed as the log of the half maximal inhibitory concentration in mol L^{-1}. [a]Unpublished data from the Koch lab.

In an attempt to elucidate the alternative pathway(s) of PAD activation, a panel of protease inhibitors was utilized in IC_{50} assays to determine the protease class(es) responsible for activation (Figure 7). Included in the panel were protease inhibitors bestatin (amino peptidases), phosphoramidon (metallo endopeptidases), E-64 (cysteine proteases), leupeptin (serine and cysteine proteases), and a complete protease inhibitor cocktail. The conclusion drawn from the previous aprotinin experiments was confirmed. Complete protease inhibition resulted in a decrease in efficacy relative to PAD alone.

Interestingly, leupeptin, and to some extent E-64, returned as positive hits in the panel, as both decreased PAD efficacy. It appears PAD activation in cell culture occurs via a combination of serene and cysteine proteases. An intriguing prospect of these results is the determination of other proteases as activation candidates. One enzyme of note is the cysteine protease cathepsin B – shown to cleave peptides after Phe-Lys sequences.[1] Cathepsin B is also associated with invasive tumors;[2] therefore, cysteine protease catalyzed prodrug cleavage may increase the scope of cancers treatable with PAD.

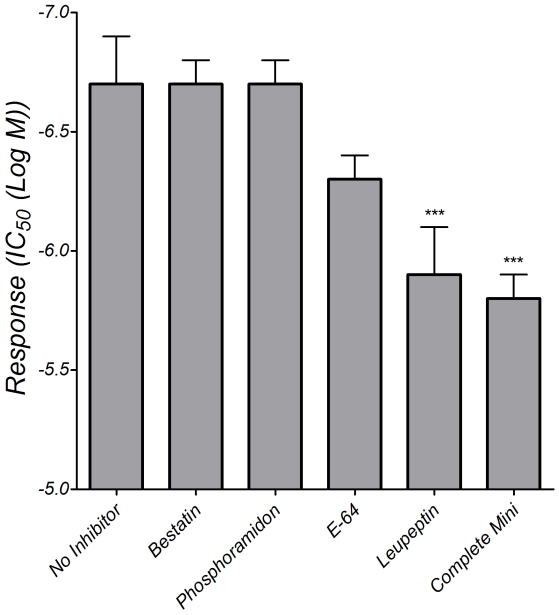

Figure 7. PAD IC_{50} values for MiaPaCa2 cell growth inhibition in the presence of a panel of protease inhibitors.
***Significant difference from no inhibitor with a p-value < 0.001.

3. shRNA knockdown of uPA and uPAR in N-HepG2 and DU-145

Although the protease inhibition panel provided insight as to a potential alternative class of proteases capable of PAD activation, the study provides little as to the direct role in PAD

efficacy assumed by plasmin and the uPA system. In order to address this, uPA and uPAR were targeted for knockdown in both N-HepG2 (liver) and DU-145 (prostate) cancer cell lines.

Knockdown was achieved using shRNA-mediated RNAi. To produce stable, permanent knockdown lines, shRNA constructs were introduced retrovirally. Constructs were selected from the Sigma MISSION database of shRNA sequences and were prepared by the Functional Genomics facility at the University of Colorado – Boulder. Two constructs per protein product were employed: shPLAU.88 and shPLAU.89 for uPA; shPLAUR.35 and shPLAUR.37 for uPAR. The targets of the constructs are mapped in Figure 8. Puromycin resistance was included in the retroviral package for selection of infected cells.

Cells were readily infected and puromycin-resistant clones were selected and grown up. Future studies will examine the expression of targeted genes in the clones and will assess their resistance to PAD treatment by IC_{50} assays.

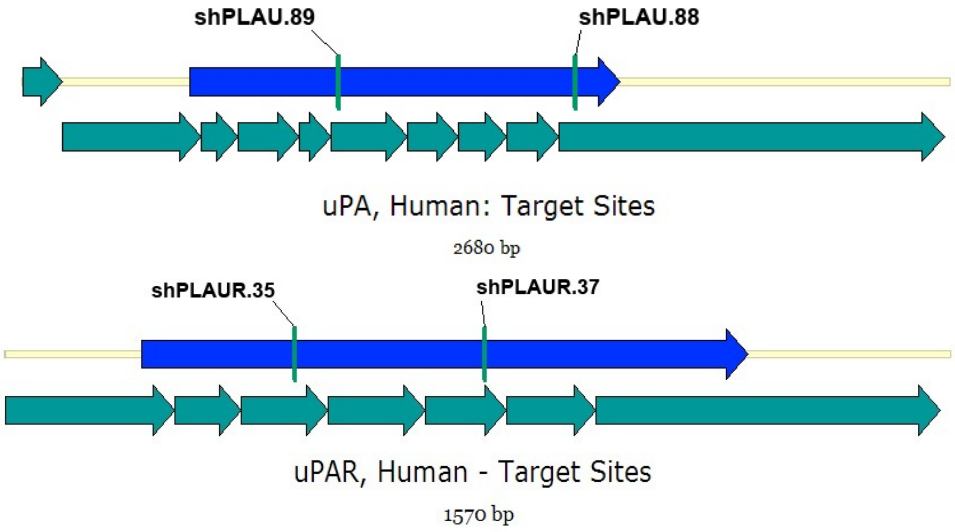

Figure 8. Target sites on uPA (top) and uPAR (bottom) mRNA of shRNA constructs. Green arrows represent exons. Blue arrows represent translated regions. Figure courtesy of Dr. Ben Barthel.

References

1. Cezari, M. H. S.; Puzer, L.; Juliano, M. A.; Carimona, A. K.; Juliano, L. Cathepsin B carboxydipeptidase specificity analysis using internally quenched fluorescent peptides. *Biochem J.* **2002**, *368*, 365-369.
2. Mohamed, M. M.; Sloane, B. F. Cysteine cathepsins: multifunctional enzymes in cancer. *Nat. Rev. Cancer* **2006**, *6*, 764-775.

Conclusion

This research offers an optimistic outlook on PAD treatment feasibility. Key intermediate **5** in a new synthetic strategy towards PAD was produced in 20% overall yield over 6 steps. Although this figure is not ideal, the simplicity of the antecedent reactions suggests optimization could dramatically increase overall yield. At the forefront of optimization is an effort towards discerning more appropriate purification techniques. Despite the purification issues, an encouraging element of the synthetic pathway is the scalable potential of each reaction. This synthesis has the capacity to provide ample material for biological assays.

This research also contributed proof of concept for targeted PAD activation by plasmin. In both timecourse and Michaelis-Menten kinetic assays, plasmin was shown to exhibit standard enzyme substrate behavior with rapid and efficient conversion when using PAD as a substrate. This activation was further observed in cancer cells. PAD treatment alone exhibited impressive cell growth inhibition with IC_{50} values at the nanomolar level, and the presence of exogenous plasmin led to an increase in efficacy of more than an order of magnitude. Though a major player, plasmin was found to be one of multiple enzymes involved in PAD activation in cell culture.

Protease inhibitor studies revealed that PAD activation is not exclusively plasmin specific. Instead, a combination of serine and cysteine proteases is responsible for prodrug activation. Further research may shed light on the specific enzymes contributing to PAD efficacy. The cysteine protease cathepsin B is of particular interest due to its known association with invasive tumors.

Due to a degree of non-specificity in protease inhibitors, the role of plasmin was probed at a more specific level. N-HepG2 and DU-145 cell lines were successfully infected with shRNA

constructs targeting mRNA of uPA and uPAR and cloned. Current experiments are in place to assay uPA and uPAR expression in knockdown clones and their resistance to PAD treatment. Resistant knockdown lines will provide a platform for future cell culture and animal studies concerning plasmin-mediated activation.

Considering the benefits of a replacement to Dox treatment, these findings are certainly encouraging. Should future animal studies reflect these promising results, PAD may prove to be a clinically valuable chemotherapeutic.

Experimental

General Remarks

Synthesis reagents were purchased from Sigma-Aldrich (St. Louis, MO) and EMD Millipore (Billerica, MA). Deuterated solvents were obtained from Cambridge Isotope Laboratories (Andover, MA). NMR spectra were obtained on a Bruker Avance-III 300 NMR Spectrometer. IR spectra were obtained using a Thermo Nicolet Avatar 360 FT-IR Spectrometer. Plasmin, protease inhibitors, and primary antibodies were obtained from Sigma-Aldrich (St. Louis, MO), Roche (Basel, Switzerland), and Santa Cruz Biotechnology (Santa Cruz, CA), respectively. Optical density measurements were made using a Hewlett-Packard 8452A Diode Array Spectrophotometer or a BioTek Instruments PowerWave X microplate reader. Reverse-phase HPLC analysis was performed using a Hewlett-Packard 1050/1100 instrument with an Agilent 4.6 x 150 mm reverse-phase column with 5 μm, C18 packing.

Abbreviations

NMR nuclear magnetic resonance, TLC thin layer chromatography, DCM dichloromethane, Dox doxorubicin, Doxaz doxazolidine, DoxF doxoform, PAD Protease-Activated Doxazolidine, DMSO dimethyl sulfoxide, HPLC high performance liquid chromatography, DIPEA N,N-diisopropylethyl amine, MeOH methanol, EtOH ethanol, DBU 1,8-diazabicyclo[5.4.0]undec-7-ene, Fmoc fluorenylmethyloxycarbonyl, KOH potassium hydroxide, HBTU *O*-(benzotriazol-1-yl)-*N,N,N′,N′*-tetramethyluronium hexafluorophosphate, HOBt 1-hydroxy-1H-benzotriazole, TFA trifluoroacetic acid, PBS phosphate buffer saline, IC50 half maximal inhibitory concentration, Koch U μM Dox min^{-1}, shRNA short hairpin RNA, uPA urokinase-type plasminogen activator, uPAR urokinase-type plasminogen activator receptor,

DMEM Dulbecco's Modified Eagle Medium, RPMI Roswell Park Memorial Institute medium, FBS fetal bovine serum, Pen/Strep penicillin-streptomycin.

1. Experimental for Steps Towards the Synthesis of PAD

4-Azidobenzyl alcohol, ***2***

As previously reported,[1] a 1.8 M solution of sodium nitrite in water (8.5 mL) was added in portions by pipet over a period of 30 min to 4-aminobenzyl alcohol (10 mmol) stirred in 5 M HCl (20 mL) at 0 ºC. Sodium azide (40 mmol) was then added in small portions over an additional 30 min at 0 ºC, allowing for N_2 effervescence. The reaction mixture was stirred for another 1 h at 0 ºC. The reaction mixture was then poured into ice water (25 mL) and basified to pH ~8 using sodium bicarbonate. Following extraction into ethyl acetate (3x25 mL washes), the combined organic layers were dried over magnesium sulfate, filtered, and concentrated via rotary evaporation at ambient temperature. The yellow oil obtained was then triturated with light petroleum to afford the desired azide as cream, needle crystals. ^{1}H NMR (300 MHz, $CDCl_3$) δ 7.37 (2H, m, Ar), 7.03 (2H, m, Ar), 4.69 (2H, d, J = 5 Hz, C*H*$_2$), 1.62 ppm (1H, t, J = 5 Hz, O*H*). 13C NMR (75 MHz, $CDCl_3$) δ 139.61, 137.79, 128.75, 119.35, 64.97 ppm. IR 2110 cm^{-1} (azide).

4-Azidobenzyl-4'-nitrophenyl carbonate, ***3***

Following the transformation reported by Griffin et al.,[1] a solution of 4-azidobenzyl alcohol (12 mmol) in DCM (100 mL) was added dropwise over 30 min to a stirred solution of 4-nitrophenyl chloroformate (12.5 mmol) and pyridine (24 mmol) in DCM (70 mL) at 0-4 ºC. The reaction mixture was stirred for an additional 72 h at room temperature until all starting materials were consumed as determined by silica gel TLC eluting with 50:50 hexanes/ethyl acetate. The DCM was removed via rotary evaporation. The resulting solid was dissolved in ethyl acetate (10

mL), washed with water (3x50 mL), dried over magnesium sulfate, and isolated via rotary evaporation. The resulting solid was then isolated via flash chromatography. ^{1}H NMR (300 MHz, $CDCl_3$) δ 8.29 (2H, m, Ar-3',5'), 7.45 (2H, m, Ar-2,5), 7.38 (2H, m, Ar-2',5'), 7.08 (2H, m, Ar-3,5), 5.27 ppm (2H, s, CH_2). ^{13}C NMR (75 MHz, $CDCl_3$) δ 155.66, 152.63, 141.22, 130.70, 125.53, 121.96, 119.74, 70.57 ppm.

Doxazolidine

An expired clinical sample of Dox•HCl (34 μmol) obtained as a lyophilized pellet containing 100 mg lactose monohydrate was dissolved in 15 mL of saturated sodium bicarbonate (pH ~8) and extracted into chloroform (20 mL) eight times. All chloroform fractions were combined, dried over sodium sulfate, filtered, and rotary-evaporated to dryness. The Dox free base was dried under high vacuum (10^{-2} Torr). The free base was then dissolved in deuterio-DMSO (15 mL) and 1.5 equiv. of prilled-paraformaldehyde was added. The mixture was stirred at room temperature under an argon atmosphere and monitored by ^{1}H NMR for completion. Upon completion, the DMSO was removed using high vacuum (10^{-2} Torr) rotary evaporation, and reaction yield was determined by anthracycline absorbance at 480 nm assuming an extinction coefficient of 11,500 M^{-1} cm^{-1}. ^{1}H NMR suggested the formation of a mixture of Doxaz and DoxF based on previous peak assignments.[2] The crude mixture was carried forward without further purification or characterization.

4''-Azidobenzyloxy carbonyl Doxaz, ***5***

Carbonate **3** (1.0 equiv.) was added to doxazolidine in 1.0 mL of DMSO. The reaction was monitored by HPLC until completion (~2 days). After diluting of the reaction mixture with 25 mL of aqueous saturated sodium bicarbonate, crude product was obtained by extraction with chloroform (8 x 10 mL). The chloroform extracts were combined and dried over sodium sulfate.

The extraction mixture was then concentrated via rotary evaporation. Isolated crude product was then subject to flash chromatography for purification. Yield and purity were determined via optical density and HPLC, respectively. ^{1}H NMR (300 MHz, $CDCl_3$) δ 13.96 (1H, s, Ar-O*H*), 13.25 (1H, s, Ar-O*H*), 8.04 (1H, m, 1), 7.80 (1H, m, 2), 7.41 (1H, m, 3), 7.36 (2H, m, 2”), 7.02 (2H, m, 3”), 5.47 (1H, t, J = 5 Hz, 1’), 5.31 (1H, s, 7), 5.13 (2H, s, Bz), 5.02 (2H, m, O-CH_2-N), 4.76 (2H, d, J = 5 Hz, 14), 4.73 (1H, s, 9-O*H*), 4.10 (3H, s, O-Me), 4.10 (3H, m, 3’,4’,5’), 3.27 (1H, m, 10), 3.02 (1H, m, 10) 3.02 (1H, t, J = 5 Hz, 14-O*H*), 2.44 (1H, m, 8), 2.29 (1H, m, 2’), 2.16 (1H, m, 8), 1.78 (1H, m, 2’), 1.36 ppm (3H, d, J = 6 Hz, 5’-Me).

N-Acetyl-GaFK(Z)-OH, ***4***

Fmoc-Lys(Z)-OH (1 mmol) was added to DIPEA (4 mmol) in 2.5 mL dry DCM. Dry DMF was added dropwise to facilitate dissolution of the amino acid. To this solution, 0.25 g 2-chlorotrityl chloride resin was added. The resulting mixture was stirred for 120 min, filtered, stirred with 95/5 MeOH/DIPEA for 30 min, filtered, and subsequently washed three times with DCM/MeOH/DIPEA (17:2:1), followed by ten iterations of alternating DCM and MeOH washes. The loaded resin was then dried *in vacuo* over KOH. Loading capacity was determined using DBU Fmoc deprotection in the absence of piperidine, monitoring the optical density of dibenzofulvene at 294 and 304 nm.

Once dry, an Applied Biosystems 433A peptide synthesizer was used for automated synthesis of the Ac-GaFK(Z)-OH tetrapeptide employing DBU and piperidine Fmoc deprotection and HBTU/HOBt activation.

Dried peptide on resin was swollen with DCM and filtered. TFA (1%) in 1.5 mL of DCM was added to the resin and stirred for 2 min. The solution was filtered through a sintered glass funnel using positive argon pressure into a flask containing 0.3 mL of 10% pyridine in MeOH.

This process was repeated 10 times, after which the resin was washed with ten iterations of alternating DCM and MeOH washes. The volume of the filtrate was reduced to 5% via rotary evaporation. Ether was added to the flask to precipitate the peptide. The ether solution was then poured off and the peptide precipitate was dried under reduced pressure. ^{1}H NMR (300 MHz, d_6-DMSO) δ 12.32 (1H, s, K-O*H*) 8.33 (1H, m, Kα-N*H*), 8.14 (1H, t, J = 6 Hz, G-N*H*), 7.99 (1H, d, J = 7 Hz, a-N*H*), 7.91 (1H, d, J = 7 Hz, F-N*H*) 7.33 (5H, m, Z-Ar), 7.23 (5H, m, F-Ar), 7.18 (1H, m, Kε-N*H*), 4.99 (2H, s, Z-CH_2), 4.50 (1H, m, K-α), 4.27 (1H, quin, J = 7 Hz, a-α), 4.06 (1H, q, J = 7 Hz, F-α), 3.67 (2H, d, J = 6 Hz, G-α), 3.09 (1H, m, K-β), 2.97 (2H, m, F-CH_2), 2.74 (1H, m, K-β), 1.83 (3H, s, Ac-CH_3), 1.72-1.35 (6H, m, K-γ,δ,ε), 0.91 ppm (3H, d, J = 7 Hz, a-CH_3).

2. Experimental for Enzymatic and Cellular Studies with PAD

2.1 Enzyme Kinetics

Plasmin timecourse

A 350 μL solution of 50 μM PAD in 5% DMSO, 95% PBS was incubated with plasmin (3.2 Koch U mL^{-1}) at 37 ºC. A 50 μL aliquot was removed at each time point (2 min, 5 min, 10 min, 30 min, 1 h, and 2 h), quenched with an equal volume of EtOH, and stored at -20 ºC. The aliquots were then analyzed using reverse-phase HPLC eluting with a gradient of 20 mM sodium phosphate pH 4.0 buffer containing 0.02% sodium azide with acetonitrile starting at 80% buffer, to 60% buffer at 5 min, to 30% buffer at 10 min, to 20% buffer at 13 min, isocratic to 15 min, to 40% buffer at 16 min, and to 80% buffer at 17 min, while detecting at 480 nm.

Michaelis-Menten kinetics

Aliquots of formulated PAD were diluted with PBS to provide the desired prodrug concentrations (10 μM, 25 μM, 50 μM, 75 μM, 100 μM, 200 μM, 300 μM, and 400 μM). Upon

addition of plasmin for a final concentration of 3.8 Koch U mL^{-1}, each aliquot was incubated at 37 ºC for 4 min, then quenched with an equal volume of EtOH and stored at -20 ºC. The mixtures were then analyzed by HPLC eluting with a gradient of 10 mM phosphate pH 4.0 buffer containing 0.02% sodium azide with acetonitrile starting at 80% buffer, to 60% buffer at 5 min, to 50% buffer at 8 min, isocratic to 9 min, and to 80% buffer at 11 min, while detecting at 480 nm.

2.2 Cancer Cell Growth Inhibition

General IC50 assay

Cells were plated in 96 well plates at ~1000 cells per well and incubated overnight. Growth media (RPMI or DMEM with 10% FBS and 1% Pen/Strep) was replaced with serum free media containing various PAD concentrations for a 24 h treatment period. Treatment media was then replaced with fresh, complete media, and the cells were left to grow for 5 days or to ~80% confluence. Cells were then fixed with 5% formalin in PBS and quantified by uptake of crystal violet. Solubilized in 4:1:1 EtOH/MeOH/water, crystal violet optical density was measured at 588 nm. Each drug condition was repeated six times, and each experiment was duplicated.

In specified experiments, exogenous enzyme was administered in the treatment media at a concentration of 3.8 Koch U mL^{-1}. Protease inhibition experiments were performed by addition of inhibitors to treatment media in IC_{50} assays. The inhibitors and their concentrations used were as follows: a total protease inhibitor cocktail (Complete Mini, Roche) made to 1x according to the manufacturer's instructions, 28 μM E-64 (cysteine proteases), 10 μM leupeptin (serine and cysteine proteases), 600 μM phosphoramidon (metallo endopeptidases), and 130 μM bestatin (amino peptidases).

3. Experimental for shRNA knockdown of uPA and uPAR in N-HepG2 and DU-145

Retroviral infection

Retroviral supernatants for each of the 6 shRNA constructs were ordered from Sigma's MISSION shRNA program and viral supernatants from the Functional Genomics Facility at the University of Colorado – Boulder. Cells were grown to ~50% confluence in 6-well plates then incubated with a retroviral cocktail of two-thirds DMEM, one-third retroviral supernatant containing 4 μg mL^{-1} polybrene. After 24 h the media was removed and the cells were incubated for a further 48 h in fresh DMEM. To select infected cells, puromycin was administered with an in-well concentration of 5 μg mL^{-1} for an incubation period of 24 h. Resistant cells were split and plated on 10 cm plates at 100 cells per plate for cloning. Clone colonies were then harvested for knockdown screening.

References

1. Griffin, R. J.; Evers, E.; Davidson, R.; Gibson, A. E.; Layton, D.; Irwin, W. J. The 4-azidobenzyloxycarbonyl function; application as a novel protecting group and potential prodrug modification for amines. *J. Chem. Soc.* **1996**, 1, 1205-1211.
2. Post, G. C.; Barthel, B. L.; Burkhart, D. J.; Hagadorn, J. R.; Koch, T. H. Doxazolidine, a proposed active metabolite of doxorubicin that cross-links DNA. *J. Med. Chem.* **2005**, 48, 7648-7657.